ISSN 1392-1207. MECHANIKA. Vol. 29, No. 5, 2023: 405–413

Research on Bionic Hierarchical Optimization of Wing Based on PLSR and PSO

Xiaoxin Zhang*, Qi Wang**
**College of Aircraft Engineering, Nanchang Hangkong University, Nanchang 330063, PR. China, E-mail: zxx9782@163.com*
***College of Aircraft Engineering, Nanchang Hangkong University, Nanchang 330063, PR. China, E-mail: wangqi439@126.com*

https://doi.org/10.5755/j02.mech.33329

1. Introduction

Modern aircraft design will be one of the main goals to reduce the aircraft's empty weight, and the lightweight design of the aircraft is also an important indicator to evaluate the performance of an aircraft. Making the spatial design layout more flexible based on the original structure to improve the overall structural load-bearing efficiency and rational structural lightweight design is the critical research point to be considered in the future development of supersonic technology [1]. As the most critical component of the aircraft, the wing provides enough lift for a successful flight and guarantees the flight's stability [2]. The layout of wing's internal structure not only greatly influences the wing's strength and stiffness, but also directly affects the aerodynamic characteristics of the aircraft.

The aircraft design process is divided into three stages [3]: conceptual design, preliminary design, and detailed design. The optimization of aircraft wings is also generally centered on these three stages. Two main engineering approaches for mixed optimization problems, like the optimization of wing or Thin-walled structures, that contain layout and dimensional design variables, are hierarchical optimization strategy and holistic solution method. The hierarchical optimization strategy separates the two variables that optimize the position and size based on the layout optimization design. However, the coupling relationship between the two variables needs to be considered more, which leads to the structure falling into a local optimum with low accuracy. The holistic solution method can obtain the global optimum solution of the optimization problem, but it is difficult to converge and takes more time when dealing with multiple variables. A hierarchical optimization method was proposed by Deng Y. [4] for the hybrid optimization problem of the wing. He first finds the optimal number and position of wing beams by the topology optimization method. Then he carries out the detailed design of the wing by dimensional optimization method according to the topology optimization result. V. J. Savsani and G. G. Tejani [5] studied the problem of simultaneous topological and dimensional optimization of truss structures under static and dynamic constraints. The optimization results of four metaheuristic algorithms are compared, and an improved algorithm based on random variation is proposed. Felipe et al. describe the shape and topological information of the structure with level-set functions, consider the effect of material properties, and propose a shape, topology, and material simultaneous optimization method [6]. Locatelli D. [7] used curved wing beams and ribs to design an aircraft wing box and investigated the advantages of curved beam ribs to achieve a more efficient load-bearing mechanism.

These hierarchical optimization approaches reduce the complexity of the problem by decomposing the structural optimization into different levels of optimization problems. However, the lack of coupling between the layout and dimensional variables design affects the optimization results. In addition, the computational effort increases significantly when the optimization level reaches three or more levels [8].

Engineering bionics is also an efficient approach to the design of aircraft. A new bio-inspired topology and shape optimization procedure for the optimization of aircraft lifting surfaces was proposed by Kolonay R. [9]. This approach is applied to improve the final structure design and subsystem layout. In terms of the design of the structure for bionic layout, Cen H. [10] designed a bionic wing structure with better performance than its prototype by referring to the constructional characteristics of the leaf vein branches. Ngoc San Ha [11] combined the advantages of bionics and proposed a new bionic sandwich panel based on the microstructure of woodpecker beaks, which provides an idea for the design of a lightweight plate hollow sandwich structure with efficient energy absorption capacity like an aircraft wing provided ideas.

In this paper, a combination of engineering bionics and hierarchical optimization design is applied to lightweight structural research. A strategy for the bionic hierarchical optimization design for the overall layout of the structure is proposed. The diatom Arachnoidiscus [12], with excellent mechanical properties, is used as a bionic template to improve the efficiency of structural optimization calculation iterations by using a data-driven agent optimization approach [13] to reasonably optimize the internal structure of aircraft wings and reduce the overall weight of the structure.

2. Bionic hierarchical optimization

In this paper, a new wing optimization process, bionic hierarchical optimization, is adopted for a more rational layout of the wing's internal structure. The topology optimization technique is used to initially determine its layout form [4] and combined with the advantages of bionics [14-15], the internal layout is post-processed to find the bionic structure layout that meets the requirements of strength and stiffness, and then the data-driven agent model optimization approach is used to optimize the overall structure in detail so that the overall structure can reach the best state and meet the requirements of practical applications. Combined with relevant optimization design concepts, a flow of bionic hierarchical optimization design for the overall layout of the structure is proposed as follows.

The topology optimization method seeks the optimal form of material distribution of the structure under load while satisfying the structural strength and stiffness, which can effectively predict the overall layout planning of the structure and provide a preliminary orientation on the overall detailed design in terms of shape as well as dimensions [16]. Therefore, topological optimization of the original structure and analysis of the internal force transfer paths of the structure when subjected to external loads eliminates the over-design problem in traditional empirical design. The next step of design optimization is based on the resulting new structure.

Since the primary method of topology optimization is to divide the design area of the original structure into finite units and to delete the units with low utilization using algorithms. Therefore, for the topology optimization of most structures, the material is always concentrated near the fixed end of the structure. In contrast, no or little material is occupied elsewhere, and this material distribution is not in line with the practical application of engineering. Therefore, the structural layout of this part needs further design.

Based on the abovementioned topology optimization problems, the topology-optimized structure is used as a basic template to find organisms with similar structures or functions in nature and analyze them. Taking the actual problem as the starting point, we take the biological forms in nature as the inspiration for imitation, combine the advantages of bionics to carry out reasonable post-processing on the topology-optimized structure, find the overall structural layout form which is more in line with the engineering reality and meets better performance requirements.

After determining the final topological shape of the structure and the location of the material arrangement through topology optimization and bionic design, the model is parametrically constructed. The data-driven agent optimization approach is introduced to determine the specific location and the dimensions of the internal structure in order to achieve the final optimal detailed design of the structure [17].

The steps needed of bionic hierarchical optimization is shown in Fig. 1.

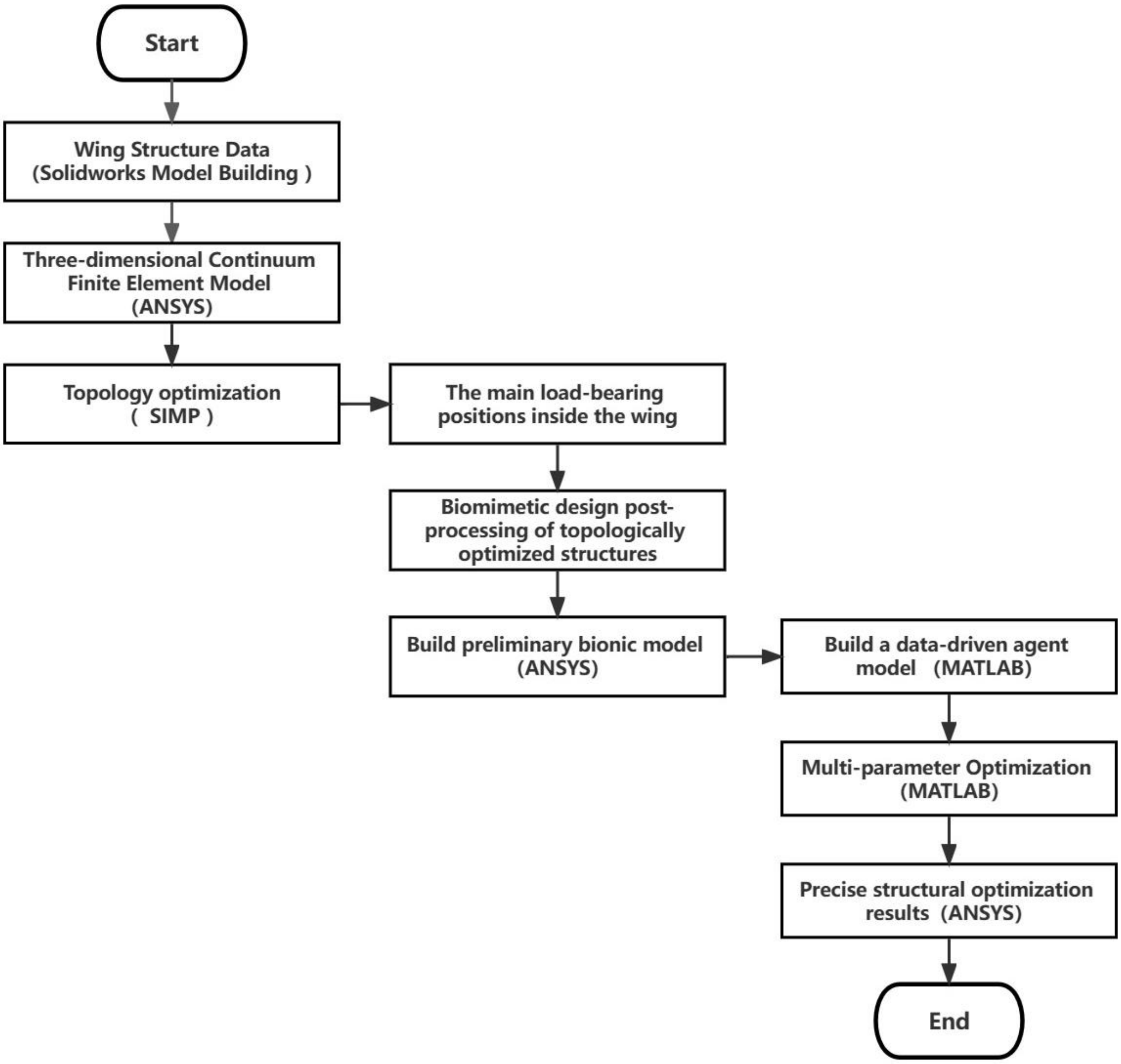

Fig. 1 The steps needed for bionic hierarchical optimization

3. Supersonic wing modeling and static analysis

3.1. Establishment of finite element model

A generic supersonic fighter wing is used as an example [7], and the idea of bionic hierarchical optimized design is introduced and applied to the example. In Fig. 2, the planar configuration and internal structure distribution of a wing with nine straight beams and nine straight ribs is shown, whose beam rib size is 7 mm. The material of the wing is Al2124-T851, according to the data provided by Lockheed Martin, and the performance parameters of the material are shown in Table 1.

Table 1

Aluminum alloy 2124-T851 properties

Young's modulus, *E*	73100 MPa
Poisson's ratio, *v*	0.33
Density, σ	2768 Kg/m^3
Yield stress, σ_y	440 MPa

In finite element analysis, the most severe load applied to the structure is often analysed to ensure that the structure can be applied to any situation. Due to lack of CFD generated loads, uniform pressure distribution corresponding to a wing load of 73100 MPa and load factor η = 9, is applied.

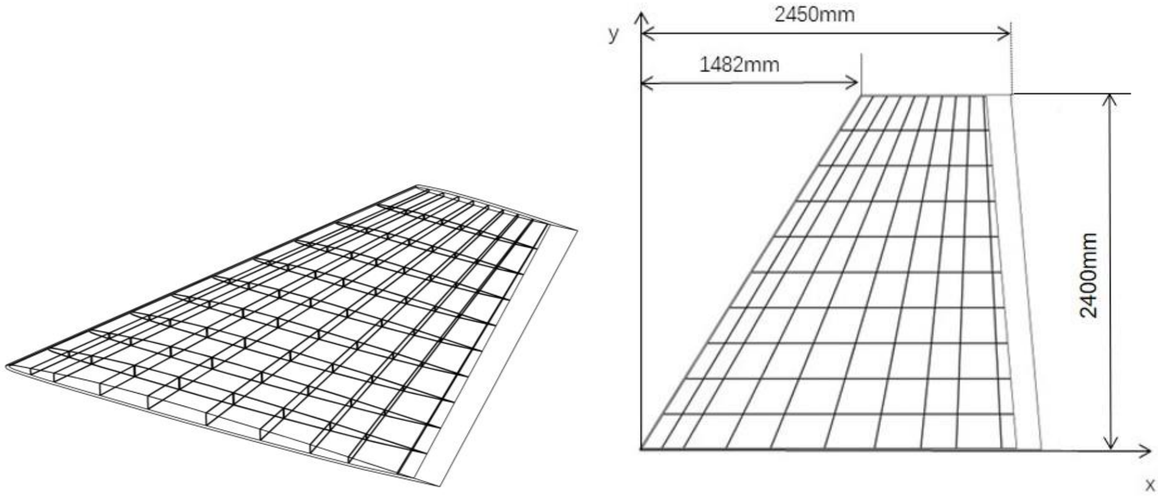

Fig. 2 Generic supersonic fighter wing geometry and internal topology

3.2. Static analysis

The static analysis of the supersonic fighter wing structure is shown in Fig. 3. The mass of the original wing box is 282.75 kg, the maximum stress value of the structure is 423.69 MPa, and the maximum deformation is 196.21 mm under the above load. It can be seen from the stress cloud diagram that the maximum equivalent stress point of the original structure appears large at the fixed surface of the structure, which is close to the yield stress limit of the material. There are multiple stress concentrations at the combination of the beam and the skin.

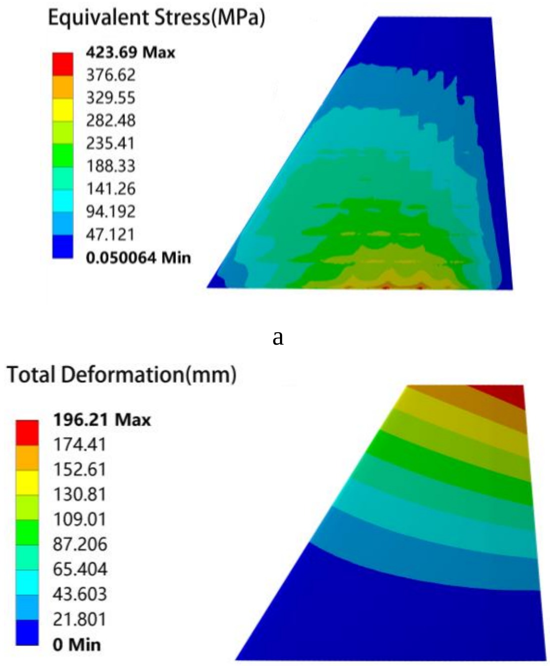

b

Fig. 3 Static analysis of the original wing: a) equivalent stress contour plot of the original supersonic fighter wing; b) total deformation contour plot of the original supersonic fighter wing

4. Conceptual design of wing internal structure

Topology optimization is an effective method for determining the structural layout and reducing the weight of a structure during the conceptual design phase. In the last few decades, researchers have provided various applications of topology optimization for various engineering disciplines [18]. A solid plate with the exact same external dimensions as the original wing is built. The solid plate is topologically optimized according to the loading and constraints of the wing. With the variable density method, the more inefficient cells subjected to forces are subtracted, and the more efficient cells subjected to forces are retained to seek the optimal performance index of the structure. In this experiment, the interior of the solid plate is selected as the optimization area, the upper and lower skins are the conformal area, and the retained structural mass is set to 20% of the mass of the solid plate.

In the new structure generated by using the topology optimization method, only the cells with relative densities between 0.6 and 1 are retained because the structural cells with relative densities below 0.6 play a relatively minor role in supporting the structure. As shown in Fig. 4, retaining the gray part. In contrast, the red part of the figure indicates the deleted materials. It can be seen with the force transmission paths within the structure when the plate material is subjected to the load applied to the wing. As seen in Fig. 4, the maximum material accumulation of the topologically optimized structure is mainly concentrated at the centre of the fixed surface. It is distributed radially outward, with several tendons extending outward from the fixed surface.

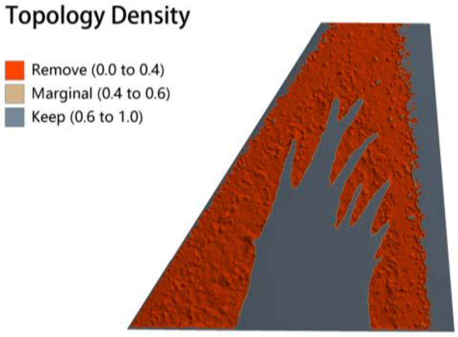

Fig. 4 Internal cross-sectional view of the topologically optimized wing structure

5. Bionic-optimized design

5.1. Biomimetic design based on diatom Arachnoidiscus shell structure

The diatom structure [12] is a single-celled organism with a fine structure, and the cell wall (siliceous shell) is mainly composed of amorphous silica. Part of the diatom shell is a particular reticular structure. It has many micropores, which makes it have excellent mechanical properties, can effectively relieve pressure, and can withstand considerable pressure. As a type of diatom (Fig. 5), the diatom Arachnoidiscus shell, from the viewpoint of mechanical properties, has a radial ridge and circumferential annular ridge distributed on its surface to form a mesh structure. The annular ridge at the centre of the diatom is more densely distributed and gradually increases in spacing outward, which can better realize the partitioning and layered transfer of load [19].

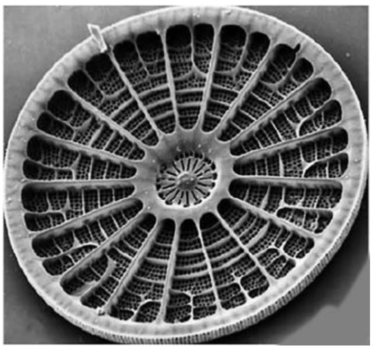

Fig. 5 The Arachnoidiscus diatom shell

Based on the excellent mechanical performance characteristics of the diatom Arachnoidiscus structure, the topologically optimized structure is used as a benchmark for the bionic design of the internal layout of the wing. As shown in Fig. 6, the diatom Arachnoidiscus structure is imitated with radial tendons and curved beams to simulate the bionic structure. Similar to the distribution of the circumferential annular ridge of the diatom Arachnoidiscus structure, the curved beams are arranged more closely in the material concentration area formed by the topology optimization. The arrangement of curved beams along the wing span direction adopts a dense inner and sparse outer way. Some radial tendons are added to the left side of the material distribution-free part in the topology optimization result to ensure more in line with the engineering reality. Due to the increase in the number of internal structures, the size of the beam ribs is reduced to 6.5 mm to keep the structural mass approximately equal to that of the original wing box and facilitate the performance comparison with the original wing box.

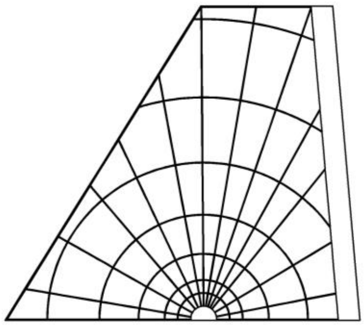

Fig. 6 Biomimetic design of the internal structure distribution

5.2. Static analysis of the bionic wing

The original wing load was applied to the bionic wing, and a static analysis was performed. The results (Fig. 7) show that, with essentially constant mass, the max-

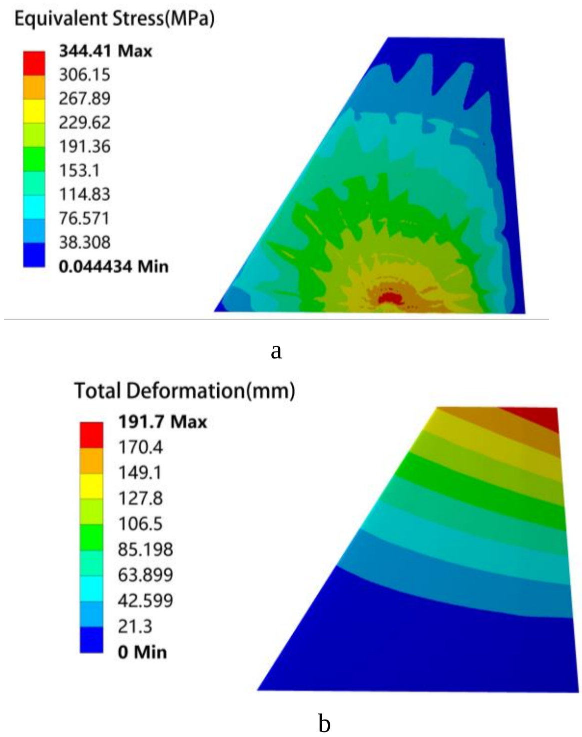

Fig. 7 Static analysis of the bionic wing: a) equivalent stress contour plot of bionic wing; b) tTotal deformation contour plot of bionic wing

imum stress value of the bionic structure is 344.41 MPa, which is 18.71% lower compared to the maximum stress value of the original structure (Fig. 3), and the maximum deformation is 191.7 mm, which is 2.30% lower compared to the maximum deformation of the original structure.

The bionic structure can effectively provide design margin for the subsequent structural optimization. The results (Fig. 7) show that the maximum stress of the bionic structure decreases by 18.71%, and the maximum deformation decreases by 2.30% with essentially the same mass.

6. Detailed optimization of position and size based on PLSR-MOPSO

Partial Least Squares Regression (PLSR) is used in this paper as a fitting mapping method, which necessarily solves approximate functional relationships. However, at the same time, Partial Least Squares also have the function of correlation analysis between variables and dimensionality reduction of data. This method solves the problem of independent variable covariance in traditional multiple regression fitting methods by reducing the number of non-primary units that do not have helpful information for the final regression results. The selection of the feature vectors focuses on the predictive effect of the independent variables on the dependent variable while reducing the number of noise points that do not contribute to the main regression results. This approach achieves the goal of reducing the number of variables included in the regression model while still ensuring the accuracy of the model [20].

In the detailed design stage, the diameter position of all ring beams from the centre of the circle, the angular position between the diagonal straight ribs, and the thickness of each beam rib were used as design parameters, resulting in a total of 36 design parameter variables. The angular positions X_1-X_{10} between the diagonal ribs between the ring beams and the distance parameters X_{11}-X_{17} are shown in Fig. 8. The thickness parameters of ring beams are X_{18}-X_{24} from outside to inside. The thickness parameters of diagonal ribs are X_{25}-X_{36} from left to right, respectively. Because the large number of variables included in the design, may cause a great workload in selecting the test sample points, the computational effort can be appropriately reduced by partial least squares regression, and the required regression accuracy can be guaranteed.

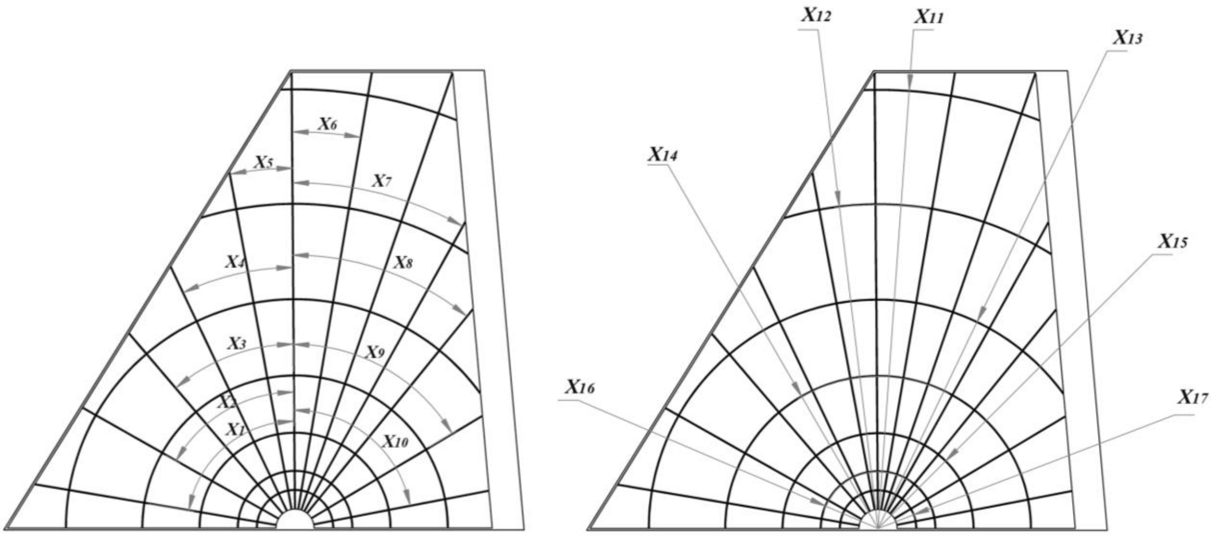

Fig. 8 Ionic wing design parameters definition

Seventy sets of initial test sample points were selected using a random sampling method, and the test sample points were introduced into the PLSR algorithm as fitted samples after finite element calculations were performed. The three fitted polynomials for the structural mass, maximum stress, and maximum deformation were obtained.

$$Y_{mass} = 340.3574 + 0.4756\times X_1 - 0.2780\times X_2 - 1.1765\times X_3 - 1.2751\times X_4 - 1.4440\times X_5 - 0.3916\times X_6 + 0.0665\times X_7 - \\ -0.2052\times X_8 + 0.4469\times X_9 - 0.4614\times X_{10} + 0.0075\times X_{11} + 0.0085\times X_{12} + 0.0032\times X_{13} - 0.0023\times X_{14} + 0.0149\times \\ \times X_{15} + 0.0065\times X_{16} + 0.0608\times X_{17} - 0.9819\times X_{18} + 0.0883\times X_{19} + 1.0225\times X_{20} - 0.7871\times X_{21} + 1.4052\times X_{22} + 0.1686\times \\ \times X_{23} - 0.8116\times X_{24} - 0.0494\times X_{25} - 1.2658\times X_{26} - 2.5609\times X_{27} - 2.8251\times X_{28} + 0.3063\times X_{29} - 0.4025\times X_{30} + 0.1638\times \\ \times X_{31} - 0.1278\times X_{32} + 0.1180\times X_{33} + 0.4567\times X_{34} - 1.4287\times X_{35} - 0.1596\times X_{36},$$

$$Y_{stress} = 255.8868 + 0.0159\times X_1 - 0.0016\times X_2 - 0.0078\times X_3 - 0.0047\times X_4 - 0.0233\times X_5 - 0.0343\times X_6 - 0.0264\times X_7 - \\ -0.0101\times X_8 - 0.0119\times X_9 - 0.0008\times X_{10} - 0.0003\times X_{11} - 0.0005\times X_{12} - 0.0016\times X_{13} + 0.0006\times X_{14} + 0.0015\times X_{15} + \\ +0.0015\times X_{16} + 0.0019\times X_{17} - 0.0789\times X_{18} + 0.1501\times X_{19} + 0.3492\times X_{20} + 0.4376\times X_{21} + 0.3326\times X_{22} + 0.1985\times \\ \times X_{23} + 0.1402\times X_{24} + 0.2813\times X_{25} + 0.2598\times X_{26} + 0.2645\times X_{27} + 0.2846\times X_{28} + 0.3340\times X_{29} + 0.3876\times X_{30} + 0.3618\times \\ \times X_{31} + 0.3095\times X_{32} + 0.2307\times X_{33} + 0.1872\times X_{34} + 0.1330\times X_{35} + 0.1371\times X_{36},$$

$$Y_{deformation} = 197.5230 + 0.0113\times X_1 - 0.0023\times X_2 - 0.0009\times X_3 + 0.0069\times X_4 + 0.0128\times X_5 + 0.019\times X_6 + 0.0451\times X_7 + 0.0065\times X_8 + 0.0135\times X_9 - 0.0012\times X_{10} - 0.0001\times X_{11} + 0.0001\times X_{12} + 0.0003\times X_{13} + 0.0004\times X_{14} - 0.0002\times X_{15} - 0.0007\times X_{16} - 0.0003\times X_{17} - 0.0045\times X_{18} - 0.0128\times X_{19} - 0.0280\times X_{20} - 0.0766\times X_{21} - 0.0956\times X_{22} - 0.0707\times X_{23} - 0.0541\times X_{24} - 0.0334\times X_{25} - 0.0551\times X_{26} - 0.0618\times X_{27} - 0.0764\times X_{28} - 0.0766\times X_{29} - 0.1622\times X_{30} - 0.1891\times X_{31} - 0.1745\times X_{32} - 0.1164\times X_{33} - 0.0851\times X_{34} - 0.0373\times X_{35} - 0.0246\times X_{36}.$$

As seen in Figs. 9 and 10, the prediction errors of the final PLSR-fitted polynomials for the maximum stress values at the test sample points ranged from 0.49% to 3.79%. The prediction errors for the maximum deformation ranged from 0.004% to 0.05%. The prediction errors for mass ranged from 0.01% to 0.05%. The prediction regression values for the maximum stress, maximum deformation, and mass were *R*1= 0.9321, *R*2=0.9828, and *R*3=0.9980, indicating that the partial least squares fitting accuracy is great.

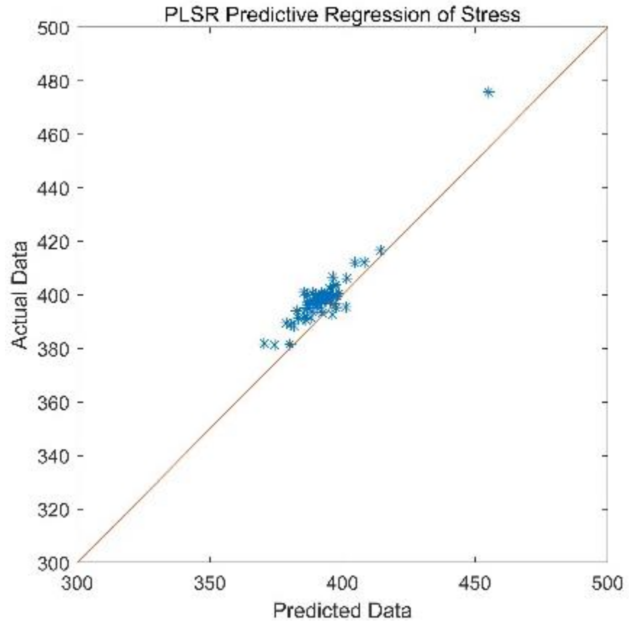

a

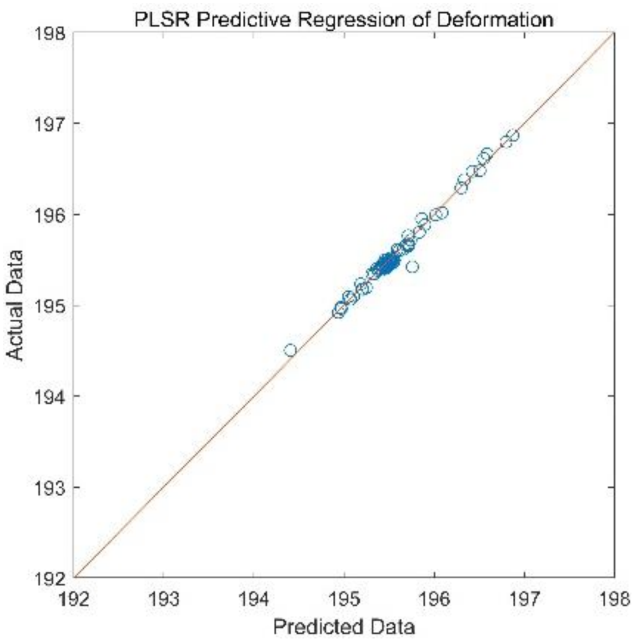

b

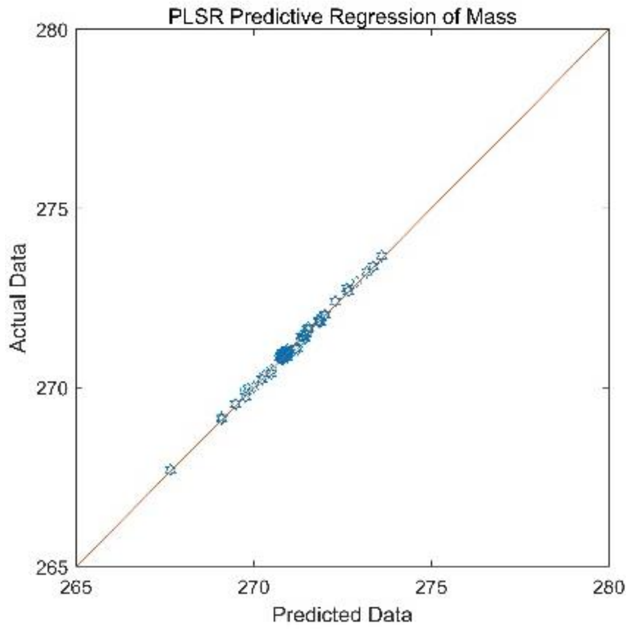

c

Fig. 9 a) PLSR predictive regression of stress; b) PLSR predictive regression of deformation; c) PLSR predictive regression of mass

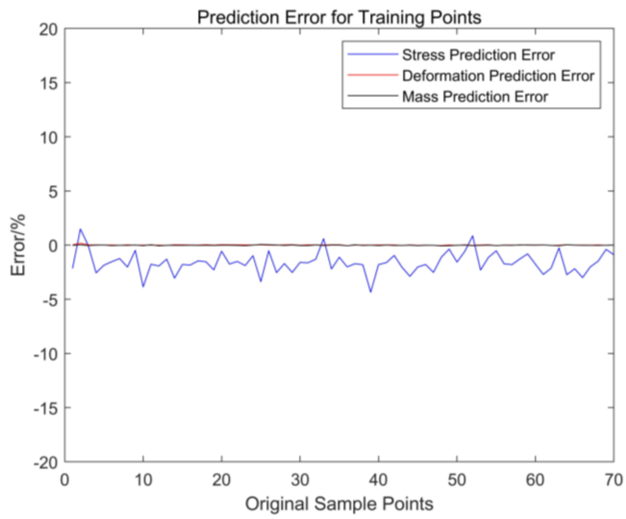

Fig. 10 Prediction error of PLSR for sample points

6.2. Particle swarm optimization algorithm

Particle Swarm Optimization (PSO) is an optimization algorithm proposed by Kennedy and Eberhart [21]. The behavioral trajectory of birds or fish in search of food is used as the basic criterion for the algorithm's operation. This collaborative movement can effectively guide the group to the best foraging place. Compared with other traditional optimization algorithms, the particle swarm optimization algorithm is simple to read, requires fewer parameters to be adjusted, and can reach convergence quickly.

The multi-objective optimization problem has multiple and conflicting objective functions, so there is no unique optimal solution to make all the objective functions optimal, and several sets of optimal solutions are often obtained. The Pareto frontier results are shown in Fig. 11 after balancing and filtering the set of optimal solutions.

The points with minimum stress, minimum deformation, and minimum mass among the generated Pareto fronts were selected for analysis, as shown in Table 2.

The layout with the bionic multilevel optimized design is constrained by the maximum stress and maximum deformation of the original wing with the minimum mass as the target. As can be seen from Table 3, the overall mass of the wing structure is reduced by 17.03 kg, which is 6.00% lower than the original structure. The final optimized structure is shown in Fig. 12.

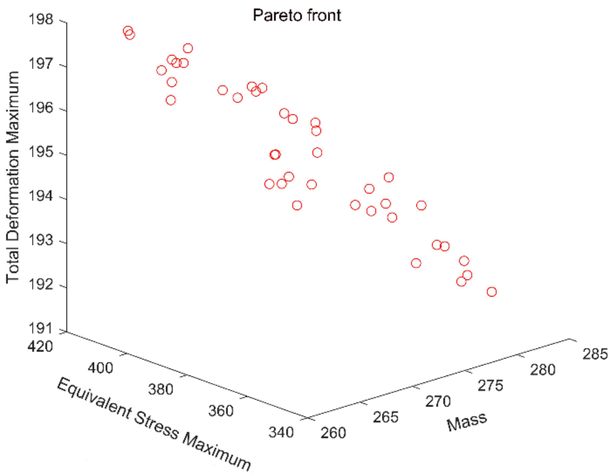

Fig. 11 MOPSO result

Table 2

The three sets of Pareto optimal solutions obtained from the optimization search

	The lowest stress	The lowest mass	The lowest deformation
X_1	78.697	75.273	80.415
X_2	61.264	55.441	63.105
X_3	38.721	36.457	41.708
X_4	26.731	25.716	27.037
X_5	11.769	8.1882	10.823
X_6	11.412	8.6998	11.302
X_7	27.626	27.767	30.046
X_8	39.71	39.135	40.877
X_9	59.353	55.185	58.612
X_{10}	80.692	75.273	80.818
X_{11}	4408.3	4451.7	4423.3
X_{12}	3203.3	3105.7	3356.2
X_{13}	2270.4	2461.5	2308.6
X_{14}	1754.7	1485.5	1487.2
X_{15}	1060.3	905.77	1095.7
X_{16}	632.89	581.12	651.75
X_{17}	436.23	383.51	426.44
X_{18}	5.1963	3.4225	5.435
X_{19}	1.8733	3.8729	3.7735
X_{20}	1.7139	1.5193	2.7735
X_{21}	2.8415	1.1373	1.4421
X_{22}	7. 8373	1.7721	7.9116
X_{23}	7. 7383	4.2122	7.8546
X_{24}	7.3067	7.3183	7.5654
X_{25}	6.9474	3.0915	6.5635
X_{26}	6.7169	1.1359	7.7268
X_{27}	7.4802	1.712	7.4264
X_{28}	7.5231	1.7287	7.5489
X_{29}	6.1597	1.9261	6.4961
X_{30}	7.4404	4.3517	7.4247
X_{31}	7.4617	5.3874	7.0811
X_{32}	7.7632	5.2793	7.9917
X_{33}	7.8075	5.7038	7.3622
X_{34}	7.6166	3.8092	7.8561
X_{35}	5.2605	3.7258	6.0563
X_{36}	7.3357	2.7753	7.5395
Predicted maximum stress	342.5625	398.1822	342.8491
Finite element analysis of maximum stress	337.5	413.12	337.69
Predicted maximum deformation	191.5192	195.9947	191.4281
Finite element analysis of maximum deformation	191.44	195.86	191.33
Predicted mass	282.2918	266.6037	282.5897
Actual Mass	282.51	266.72	282.13

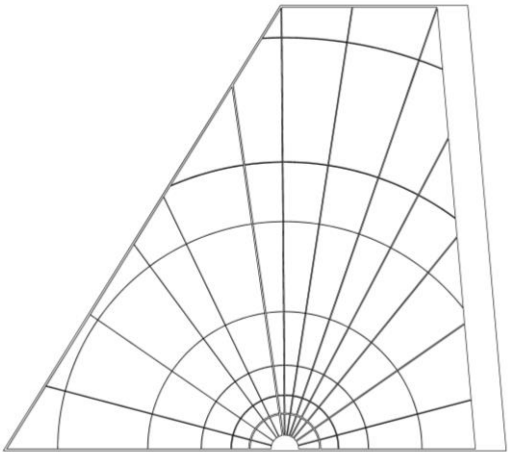

Fig. 12 Final optimized structure of the internal layout of the wing

Table 3

Comparison of wing performance

Structure type	Maximum stress value, MPa	Maximum deformation value, mm	Mass, Kg
Original wing	423.69	196.21	282.75
Bionic wing	344.41	191.7	281.56
Bionic wing after lightening	413.12	195.86	266.72

7. Conclusions

1. In the conceptual design stage, topology optimization is used to obtain the primary structural forms under a specific load. The main load-bearing structures are extracted according to the obtained results, which can significantly help the subsequent search for the optimal structure.

2. The preliminary bionic layout of the wing's internal structure based on the arachnoid algae structure was carried out. Compared with the original wing model, the maximum deformation and maximum stress are reduced while the overall mass remains approximately the same.

3. The fitted relational equations of mass, stress, and strain are constructed with high regression accuracy using PLSR.

4. Detailed optimization using the PSO algorithm to obtain the optimal structural parameters can further improve the optimization effect and effectively reduce the structure's mass.

This method is simple and practical, wcan be extended to the fields of weight optimization of complex plate structures.

References

1. **He, L. T.; Wan, X. P.; Zhao, M. Y.** 2008. Composite aircraft wing structure optimization using combination of layout and sizing, China Mechanical Engineering 19(17): 2077-2080 (in Chinese). https://doi.org/10.3321/j.issn:1004-132X.2008.17.014.
2. **Conway, E. M.** 2005. High-speed dreams: NASA and the technopolitics of supersonic transportation, 1945–1999. JHU Press. https://doi.org/10.2307/4486221.
3. **Raymer, D.** 2012. Aircraft design: a conceptual approach, American Institute of Aeronautics and Astronautics, Inc. https://doi.org/10.1177/026461969100900306.
4. **Deng, Y.; Zhang, W.; Zhang, Y.** 2005. Aircraft wing structural layout study based on hierarchy optimization, Structure & Environment Engineering 2005(01): 27-35+63 (in Chinese). https://doi.org/10.3969/j.issn.1006-3919.2005.01.005.
5. **Savsani, V. J.; Tejani, G. G.; Patel, V. K.; Savsani, P.** 2017. Modified meta-heuristics using random mutation for truss topology optimization with static and dynamic constraints, Journal of Computational Design and Engineering 4(2): 106-130. https://doi.org/10.1016/j.jcde.2016.10.002.
6. **Fernandez, F.; Barker, A. T.; Kudo, J**. 2020. Simultaneous material, shape and topology optimization. Computer Methods in Applied, Mechanics & Engineering 371: 113321. https://doi.org/10.1016/j.cma.2020.113321.
7. **Locatelli, D.** 2012. Optimization of supersonic aircraft wing-box using curvilinear sparibs, Virginia Tech. http://hdl.handle.net/10919/26345.
8. **Zhou, D. F.** 2019. An integrated optimization method of structural size, shape and topology, Nanjing: Nanjing University of Aeronautics and Astronautics, p. 17-18 (in Chinese). https://doi.org/10.27239/d.cnki.gnhhu.2019.000201.
9. **Kolonay, R.; Kobayashi, M.** 2010. Topology, shape, and sizing optimization of aircraft lifting surfaces using a cellular division method, 13th AIAA/ISSMO Multidisciplinary Analysis Optimization Conference, p. 9079. https://doi.org/10.2514/6.2010-9079.
10. **Cen, H.; Chen, W.** 2009. Structural bionics design and experimental analysis for small wing, Journal of Mechanical Engineering 45(3): 286-290. https://doi.org/10.3901/JME.2009.03.286.
11. **Ha, N. S.; Lu, G. ; Xiang, X.** 2019. Energy absorption of a bio-inspired honeycomb sandwich panel, Journal of materials science 54: 6286-6300. https://doi.org/10.1007/s10853-018-3163-x.
12. **Dubicki, A.; Zglobicka, I.; Kurzydłowski, K. J.** 2021. Investigation of energy-absorbing properties of a bio-inspired structure, Metals 11(6): 881. https://doi.org/ 10.3390/met11060881.
13. **Jin, Y.; Wang, H.; Chugh, T.; Guo, D.; Miettinen, K.** 2018. Data-driven evolutionary optimization: an overview and case studies, IEEE Transactions on Evolutionary Computation 23(3): 442-458. https://doi.org/10.1109/TEVC.2018.2869001.
14. **Diaz, R. C.** 2012. The ongoing bionic revolution, Current Opinion in Otolaryngology & Head and Neck Surgery 20(5): 385. https://doi.org/10.1097/MOO.0b013e328357d29e.
15. **Naleway, S. E.; Porter, M. M.; McKittrick, J.; Meyers, M. A.** 2015. Structural design elements in biological materials: application to bioinspiration, Advanced materials 27(37): 5455-5476. https://doi.org/10.1002/adma.201502403.
16. **Walker, D.; Liu, D.; Jennings, A. L.** 2016. Wing design utilizing topology optimization and additive manufacturing, 57th AIAA/ASCE/AHS/ASC Structures, Structural Dynamics, and Materials Conference, p. 1246. https://doi.org/ 10.2514/6.2016-1246.
17. **Zhang, K. S.; Han, Z. H.; Gao, Z. J.; Wang, Y.** 2019. Constraint aggregation for large number of constraints

in wing surrogate-based optimization, Structural and Multidisciplinary Optimization 59: 421-438. https://doi.org/ 10.1007/s00158-018-2074-4.
18. **Pedro, H. T. C.; Kobayashi, M. H.** 2011. On a cellular division method for topology optimization, International Journal for Numerical Methods in Engineering 88(11): 1175-1197. https://doi.org/ 10.1002/nme.3218.
19. **Hamm, C.** 2015. Evolution of Lightweight Structures: Analyses and Technical Applications (Vol. 6). Springer. https://doi.org/ 10.1007/978-94-017-9398-8.
20. **Geladi, P.; Kowalski, B. R.** 1986. Partial least-squares regression: a tutorial, Analytica chimica acta 185: 1-17. https://doi.org/ 10.1016/0003-2670(86)80028-9.
21. **Kennedy, J.; Eberhart, R.** 1995. Particle swarm optimization, Proceedings of ICNN'95-International Conference on Neural Networks, p. 1942-1948 https://doi.org/10.2514/2.2111.

X. Zhang, Q. Wang

RESEARCH ON BIONIC HIERARCHICAL OPTIMIZATION OF WING BASED ON PLSR AND PSO

S u m m a r y

The layout of the wing's internal structure not only dramatically influences the wing's strength stiffness but also directly affects the aerodynamic characteristics of the aircraft. Based on the original wing structure, a more flexible spatial design layout to achieve improved overall structural load-bearing performance, and a reasonable structural lightweight design are the research priorities to be considered for the development of future aircraft. Therefore, this paper attempted to design and analyze a lightweight airfoil that meets the performance requirements. Combining the strategy of hierarchical optimization design with the advantages of engineering bionics, the diatom Arachnoidiscus bionic structure, topological optimization, partial least squares regression (PLSR), and multi-objective particle swarm algorithm (PSO) are applied to optimize the placement and size of wing’s internal components. The simulation results show that the weight of the optimized wing structure is reduced by 6% while satisfying the requirements of maximum stress and maximum deformation.

Keywords: hierarchical optimization; engineering bionics; wing; partial least squares regression; multi-objective particle swarm algorithm.

Received February 1, 2023
Accepted October 9, 2023